

FIG. 1. Conformation of one melittin chain from the tetramer. *a*, schematic drawing of chain A (see Fig. 2) of melittin. (Drawing by Mallory Pearce.) *b*, stereo pair showing chain A in approximately the orientation in *a*. Atoms are drawn with radii equal to 15% of their van der Waals radii.

RESULTS

Polypeptide Backbone Structure and Hydrogen Bonding—

The polypeptide backbone of each melittin chain in the tetramer has the overall shape of a bent rod (31), with a bend angle of about 120° . Residues 1–10 form an α -helical structure which is connected, through the bend at residues 11 and 12, to a longer α -helix containing residues 13–26 (Fig. 1). Even in the region of the bend, however, the polypeptide backbone is in a generally helical, but not α -helical, conformation. The principal deviation from an α -helix is at the peptide group linking residues 11 and 12, which is turned about 180° away from that expected in an α -helix. The hydrogen bonding pattern for the chain other than this peptide group appears to be that of an α -helix (see Fig. 1), except, of course, that the carbonyl oxygen of Thr-10 does not hydrogen bond to Pro-14. In chain A, the amide nitrogen of Leu-13 is hydrogen bonded to the carbonyl oxygen of Leu-9 although they are on opposite sides of the bend. In chain B, the amide nitrogen of Leu-13 hydrogen bonds to the carbonyl oxygen of Val-8. We note also that because the bend in residues 11 and 12 is helical in nature, the two α -helical segments of the melittin chain match to form a helix the length of the entire bent chain.

Spatial Distribution of Apolar and Polar Amino Acid Side Chains on the Melittin Helix—Although the side chains of residues 1–6 are all hydrophobic, one side of the helix is somewhat more apolar than the other even in this region. The reason is that the bulky side chains of Ile-2, Val-5, and Leu-6 are all positioned (Fig. 1) towards the “inner” side or the “upper” side of the bent rod, while the opposite face of the helix has only the small Ala-4 chain. There is a nearly complete spatial segregation of apolar and polar side chains in residues 7–20. The most apolar residues Val-8, Leu-9, Leu-13, Leu-16, Ile-17, Trp-19, and Ile-20 are all on the inner surface

or the upper surface of the chain; the hydrophilic residues Lys-7, Thr-10, Thr-11, and Ser-18 are all on the outer surface of the bent rod. Pro-14 is the only large apolar side chain that is on the outer surface of the bent rod.

The final six residues in the chain are all hydrophilic; the four positively charged lysine and arginine side chains extend almost directly away from the backbone of the helix so that they are well separated and the entire circumference of the helix is charged in this region.

The melittin chain can thus be divided into three regions based on the distribution of polar and apolar side chains: 1) a hydrophobic NH_2 -terminal region, 2) a central section with hydrophobic and hydrophilic faces, and 3) an entirely hydrophilic C-terminal region.

Symmetry of the Tetramer—The four melittin chains in the tetramer are nearly identical in conformation. The two chains in the asymmetric unit (*chains A and B* in Fig. 2) are related by an approximate 2-fold axis of symmetry. These chains run antiparallel with their “upper” surfaces (Fig. 1) in close contact. An exact 2-fold axis of symmetry, perpendicular to the approximate one, relates chains A and B to the other two chains in the tetramer (*chains C and D* in Fig. 2), placing the “inner” surfaces of all four chains close together. The overall symmetry of the tetramer is approximately 222.

Subunit Contacts in the Interior of Tetrameric Melittin—Essentially all the subunit-subunit contacts in the melittin tetramer are hydrophobic. There appears to be no hydrogen bonding between chains and the closest charge-charge interaction is between lysines 23 of chains A and C and between lysines 23 of chains B and D. The distances between these pairs of atoms appears to be 4–6 Å, although this is uncertain since the locations of the side chains of residues 21–26 were not clear in our multiple isomorphous replacement map (28)

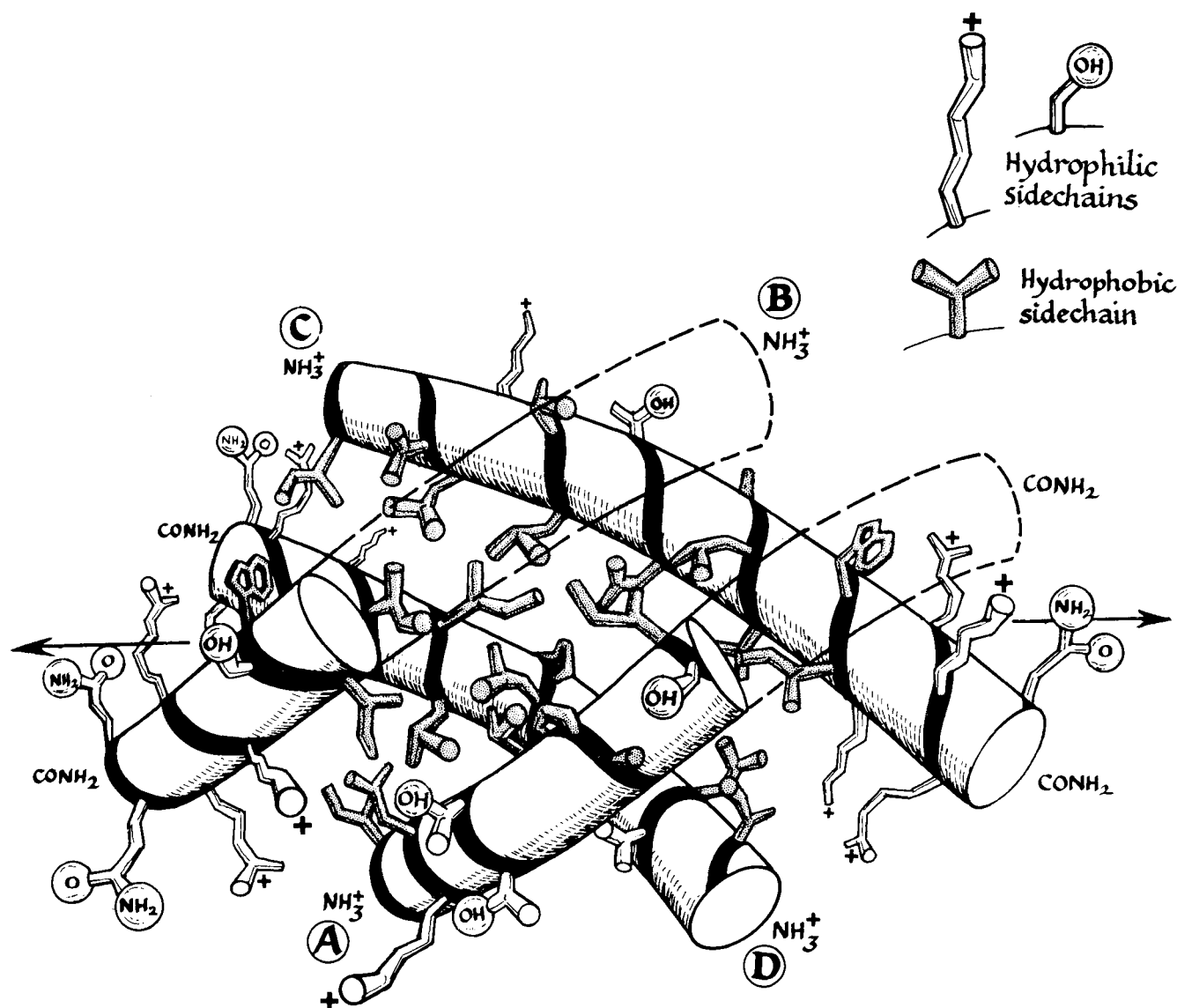


FIG. 2. Cut-away drawing showing the packing of melittin chains in the tetramer. Chain A was the chain built into our electron density map (see preceding paper, Ref. 28). Chain B is related to chain A by an approximate 2-fold axis roughly perpendicular to the page. Chains C and D are related to chains A and B by the exact 2-fold axis nearly in the plane of the page as indicated. (Drawing by Mallory Pearce.)

and have not yet been completely resolved.

As is illustrated in Fig. 2, the hydrophobic residues on the "inner" and "upper" surfaces of each melittin chain are all packed in the interior of the tetramer, which is completely apolar. In this region, the side chains of 40 valyl, leucyl, isoleucyl, and tryptophanyl residues are packed very closely together and amino acid residues from separate chains are highly interdigitated (Fig. 3A).

Since each melittin chain is mostly α -helical, the subunit-subunit contacts in the tetramer can be described in terms of helix-helix contacts. There are four distinct types of close helix-helix contacts in the melittin tetramer. Since the symmetry of the tetramer is only approximately 222, not all examples of a particular type of helix-helix crossing are identical. Fig. 4 shows the crossing angle and the intercalation of the side chains in one example of each type. It can be seen that in each case, all the side chains from the lower helix (represented by solid patches in Fig. 4) fall between the side chains of the upper helix (represented by open patches).

Melittin-Solvent Interactions—While the internal contacts in tetrameric melittin are almost exclusively between apolar

residues, the melittin-solvent interactions involve some apolar and essentially all the polar residues. Nearly all the hydrophilic side chains are at least partly exposed to the solvent by the criterion given under "Materials and Methods". (The ϵ -amino groups of the four lysines-23 are inaccessible to solvent in our model, but the positions of these side chains are quite uncertain (28).)

The highly charged C-termini of the four chains are spaced well apart and, except for the four Lys-23 side chains, all charges on neighboring chains are at least 7 Å apart. Additionally, the side chains for the Lys-7, Thr-10, Thr-11, and Ser-18 residues all point directly out into the solvent. Coupled with the symmetry of the tetramer, the result is that the polar side chains form a hydrophilic "coat" around the tetramer (Fig. 2). Of the 192 non-hydrogen atoms in hydrophilic side chains in the tetramer, 156 are exposed to solvent. In contrast, the apolar residues forming the core of the tetramer are almost completely shielded from the solvent by the hydrophilic side chains and by the polypeptide backbones; of the 198 atoms in hydrophobic side chains, only 66 are accessible to the solvent.

During the refinement of the melittin structure, we were

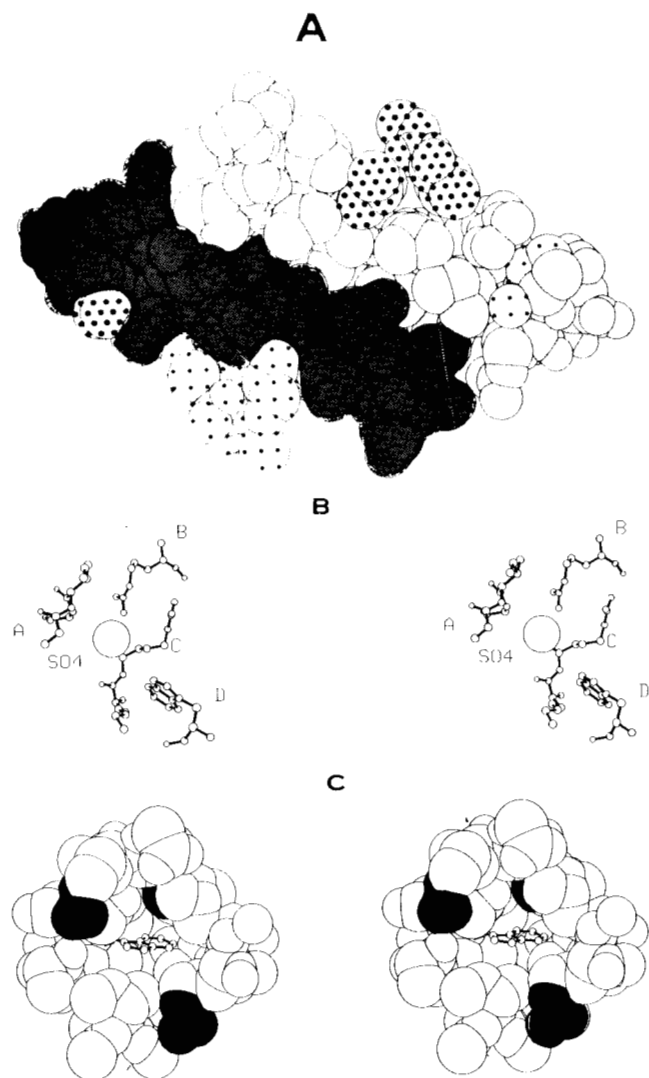


FIG. 3. The interior of the tetramer, bound solvent, and the environment of tryptophan-19. *A*, cut-away view of a space-filling (van der Waals radii) model of melittin. One-half of the tetramer is shown; there is a horizontal 2-fold axis in the plane of the page and a vertical approximate 2-fold axis. Chain *A* is shaded, chain *B* is unshaded, chain *C* has the finely spaced dots and chain *D* has the coarsely spaced dots. *B*, stereo pair showing the amino acid residues with atoms within 6 Å of solvent molecule (labeled *SO4*) bound near NH_2 terminus of chain *B*. The residues labeled *A* are Gly-1-Gly-3 of chain *B*; *B* is Arg-24 of chain *A*. *D* is Trp-19 of chain *B* in an adjacent tetramer. *C* is Lys-23 and Arg-24 of chain *B* in another adjacent tetramer. *C*, stereo pair of the atoms in the tetramer near tryptophan-19 of chain *A*. All atoms within 10 Å of C_δ of Trp-19 are shown. The side chain atoms of Trp-19 are shown with radii of 0.3 Å, all other atoms are drawn with van der Waals radii. The charged groups of one lysine and two arginine residues are shaded; a second nearby lysyl ϵ -amino group is occluded in this view. Note that the positions of these charged side chains are somewhat uncertain (see text). A bound solvent molecule related to the one shown in *B* is located toward the viewer about 3.7 Å from N_ϵ of Trp-19.

able to locate by difference map analysis several solvent molecules which are tightly bound to the melittin tetramer. One solvent molecule is located 2.6 Å from the carbonyl oxygen of Ser-18 and 3.7 Å from N_ϵ of Arg-22 in chains *A* and *C*. As discussed in the previous paper (28), this might correspond to a water molecule which is nearly always present at this site or to a sulfate or formate ion from the crystallization medium only present part of the time. One other readily identifiable solvent molecule is located near the NH_2 terminus of each chain in the tetramer. Each of these is also near the

side chains of Trp-19 and Arg-24 of chains in adjacent tetramers in the crystal and is between 3.4 and 6 Å away from a total of eight separate charged or polar groups. As discussed in the previous paper (28), these solvent molecules are probably formate or sulfate ions. Fig. 3*B* shows a model of the region near one of these ions.

Environment of the Tryptophanyl Side Chains—Because of the numerous fluorescence studies of melittin (*e.g.* Refs. 2, 9, 12), the tryptophanyl side chains are of special interest. Each of these four residues in the melittin tetramer is in contact with both polar and apolar groups (Fig. 3*C*). N_ϵ and one or two other atoms in each tryptophanyl side chain are exposed to the solvent, and the indole ring of each tryptophanyl residue is within 4–6 Å of three or four charged groups. In addition, each indole ring is in close contact with many apolar side chains.

Packing of the Tetramers in the Form II Crystals—Fig. 5 shows schematically a section perpendicular to the *c* axis one tetramer thick through a form II crystal of melittin. It can be seen that this array of tetramers is composed of two layers of dimers sandwiched together: an upper layer in which pairs of chains from each tetramer run from lower left to upper right and a lower one in which the chains run from upper left to lower right. In each layer, the end-to-end contacts between chains are very close, as are the side-to-side contacts within dimers. These end-to-end dimers form long melittin “strings.” On the other hand, the side-to-side contacts between chains not part of the same tetramer are quite distant; the closest approach between the strings of dimers is 10 Å. Thus, there are essentially no contacts within a layer holding the strings of end-to-end dimers together. Nevertheless, as each dimer in the upper layer is attached to a dimer in the lower plane through intramolecular hydrophobic contacts, the whole array of tetramers is held firmly. It may also be seen by inspection of Figs. 1, 2, and 5 that each of the two layers of chains in Fig. 5 is amphiphilic; one surface of the layer is hydrophilic (the outsides of the tetramers) and the other surface is hydrophobic (the interiors of the tetramers).

The packing of the arrays of tetramers in the *c* direction (perpendicular to the page in Fig. 5) is fairly simple. They are stacked vertically on top of each other, except that every other one is turned 180° about the *c* axis before stacking. A melittin crystal may thus be viewed as a stack of parallel protein bilayers.

DISCUSSION

Overall Design of the Tetramer—The structure of tetrameric melittin seems ideally suited for conferring high aqueous solubility on a small protein that has a predominance of apolar residues. Most of the charged and polar amino acid side chains are spread out over the surface of the tetramer; along with the polypeptide backbones of the four chains, these residues form a hydrophilic coat which shields the central core of apolar side chains from the solvent. Additionally, since the melittin tetramers contain only positive charges, the electrostatic repulsion between them probably contributes to melittin’s aqueous solubility.

The hydrophobic core of the tetramer has a “density” of about 0.74 g/cm³, similar to that of liquid decane (0.73 g/cm³, Ref. 32). The tetramer as a whole has a packing density of 0.80, that is, 80% of the space in the tetramer is within the van der Waals radius of an atom in the tetramer, and a mass density of 1.41 g/cm³. Richards (30) has calculated the packing density and mass “density” of ribonuclease S in a similar fashion; the values obtained were 0.74 and 1.29 g/cm³, respectively. The greater density of melittin may arise from its formation from four α -helical rods, without the necessity to

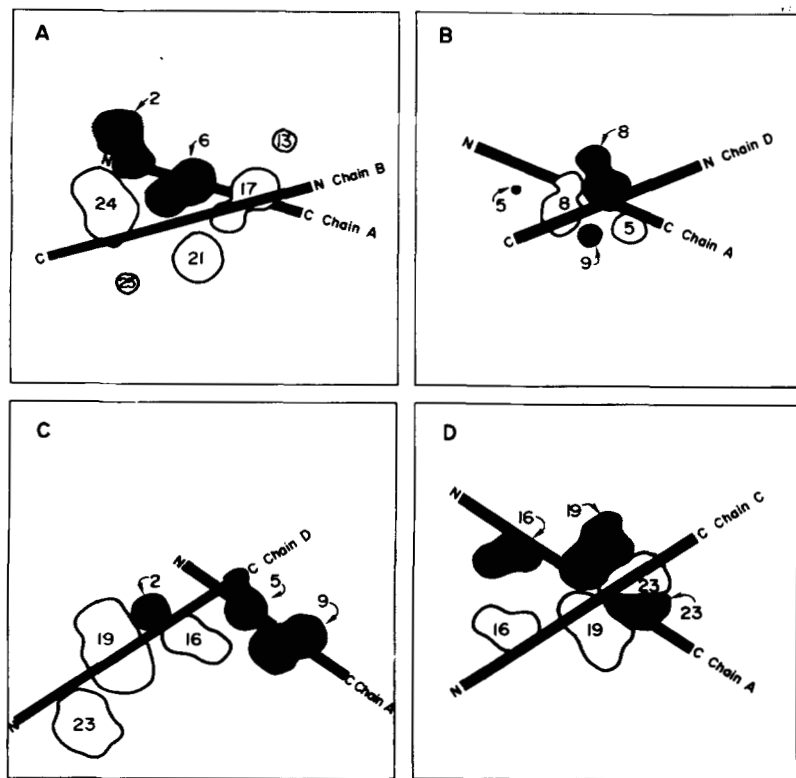


FIG. 4. Helix-helix crossings in tetrameric melittin. The axis of a segment of α -helix is represented by a solid line, the ends are labeled (*N* or *C*) to indicate the direction of the chain. Residues in the lower chain whose van der Waals envelope cross the plane midway between the helix axis are represented by solid patches, those from the upper chain are represented by open patches. The shape of each patch is the intersection of the van der Waals envelope of this side chain with the mid plane between the helix axis. Residue numbers are indicated. *A*, residues 1–11 of chain A crossing residues 13–26 of chain B. The minimum distance d between the helix axes is 11.0 Å; the interhelical angle Ω (33) is 33°. *B*, residues 1–11 of chain A crossing residues 1–11 of chain D. $d = 9.8$ Å; $\Omega = 45^\circ$. *C*, residues 1–11 of chain A crossing residues 13–26 of chain D. $d = 10.0$ Å; $\Omega = -110^\circ$. *D*, residues 13–26 of chain A crossing residues 13–26 of chain C. $d = 11.4$ Å; $\Omega = -113^\circ$.

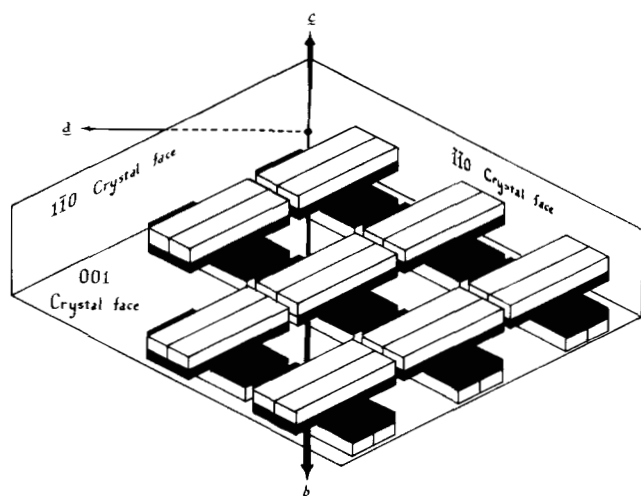


FIG. 5. Packing of melittin chains in the form II crystals. Each tetramer is schematically represented by four crossed blocks. The shaded side represents the side of the melittin chain which is hydrophobic for residues 1–20. The faces of the form II crystals are related to the packing of the tetramers. One face is perpendicular to the c axis; it is the surface of a sheet of tetramers. The other two faces are parallel to the c axis and to two of the chains in each tetramer.

incorporate lower density turns.

Helix-Helix Crossings—The tightly packed interior of the melittin tetramer is made up of one side of each of the eight α -helical segments in the tetramer. Chothia *et al.* (33) have studied the packing of pairs of α -helices and have found that there are a few patterns of helix-helix crossings which can account for nearly all of the close contacts between pairs of α -helices in ten different proteins. In these common helix-helix crossing patterns, the side chains of the two helices interdigitate in a “ridges into grooves” fashion. All four types of helix-helix crossings found in the melittin tetramer fall into

one of these patterns. *Crossing A* in Fig. 4 is a type 3–4 crossing (33) in which the ridge formed by residues 2 and 6 in the lower helix (chain A) runs parallel to the ridge formed by residues 21 and 24 in the upper helix (chain B). The crossing angle is 33°; the value suggested by Chothia *et al.* (33) for a type 3–4 helix crossing with a helix-helix distance of 11 Å is 20°. *Crossing B* is a type 3–4 “crossed ridge” packing. Residue 12 on the lower helix is a glycine, so residue 5 in the upper helix can pack directly above it (33). In this crossing, the ridges formed by residues 8 and 12 and by 5 and 9 of the lower helix pack across the ridge formed by residues 5 and 8 of the upper helix. The crossing angle in this case is 45°; the value suggested by Chothia *et al.* (33) is $\sim 55^\circ$. *Crossings C* and *D* are both type 1–4 crossings. In crossing C, the ridge formed by residues 5 and 9 of the lower helix runs parallel to that which would be formed by residues 15, 16, and 17 in the upper helix. The side chains of residues 15 and 17 in the upper helix actually do not cross the plane midway between the two helices and are thus not shown in Fig. 4. Similarly, in crossing D, residues 19 and 23 of the lower chain form a ridge running parallel to residues 18, 19, and 20 of the upper helix (but only residue 19 of the upper helix actually is in contact with the lower helix). The crossing angles for crossings C and D are -110° and -113° ; those suggested by Chothia *et al.* (33) are -109° and -114° , respectively.

Role of the Melittin Sequence—We can envision several major roles for the 5 lysine and arginine residues in the melittin chains. First, as mentioned above, the +24 charge on a melittin tetramer (including the NH_2 termini) probably helps to prevent the aggregation of melittin tetramers in solution. On a second level, the equilibrium between melittin monomers and tetramers in solution is probably affected by the six positive charges on each monomer. In solutions with physiological ionic strength and pH, tetrameric melittin is present in roughly equal proportions with monomeric melittin when the total melittin concentration is about 200 μM (3). This is about 100 times the concentration of melittin required

to produce 50% lysis of a dilute suspension of erythrocytes (4) and is probably less than 1/100 the concentration found in the venom sac of the worker bee (estimated from information in (35) and (36)). The monomer-tetramer equilibrium is probably determined by a combination of the apolar "attraction" between the hydrophobic side chains of melittin and the electrostatic repulsion of the charged side chains. Since melittin appears to be monomeric in lipid bilayers (11, 13), this equilibrium ratio between tetramer and monomer may be important to the biological function of the protein. Finally, once melittin is bound to a membrane containing phospholipids, the positive charges in melittin might interact with the phosphate groups in the lipids, binding melittin firmly to the membrane and possibly affecting the lipid structure. Habermann and Kowallek (37) have prepared a modification of melittin in which the NH₂-terminal amino and lysine ϵ -amino groups are succinylated. This modified melittin was substantially less lytic than melittin, although it was not shown that this was caused directly by the substitution of negative for positive charges.

Proline-14 may contribute in several ways to the formation of the bend in the melittin chain although it is actually part of the second α -helical region of the chain. First, since Pro-14 does not form a hydrogen bond to Thr-10, the α -helix is destabilized between residues 10 and 14. Second, the atoms in the proline side chains would be very close to the carbonyl oxygen atom of Thr-10 if the chain remained in an α -helical conformation. The formation of the bend relieves this close contact. One should note, however, that DeGrado *et al.* (15) have found that a synthetic melittin analog which does not contain proline forms a tetramer in aqueous solution.

An effect of the bend at residues 11 and 12 in each melittin chain is to allow more contact between the melittin chains than would otherwise be possible. This may be understood by noting that if all four chains were straight α -helices, each side-by-side pair of chains would have some point of close contact and would diverge from that point (34) (unless all chains run parallel, in which case the side chains from separate helices cannot pack closely together according to the model of Chothia *et al.* (33)). In the melittin tetramer, each pair of side-by-side chains has two close contacts because the bend allows the helices to cross in two places. Consequently, all four chains are in close proximity throughout residues 1-20.

Possible Folding Pathway from Monomeric to Tetrameric Melittin—Lauterwein *et al.* (38) have studied monomeric melittin in aqueous solution using nuclear magnetic resonance methods and have found that although monomeric melittin is predominantly in a flexible extended (non- α -helical) form, residues 5-9 and 14-20 are more highly structured than the rest of the chain. They suggested that these two hydrophobic segments might serve as nucleation centers in the folding of monomeric melittin into tetramers. Upon inspection of our model, we note that nearly all the residues involved in subunit-subunit contacts in the melittin tetramer are contained in these two segments (see Fig. 4). Each chain of melittin makes contact with one other chain at both of these segments and with each of the other two chains at one or the other of these segments.

We suggest that the folding pathway from monomeric to tetrameric melittin might consist of the formation of α -helical structures in residues 5-9 and 14-20 with a flexible hinge in residues 10-13, followed by contact and adhesion of the hydrophobic side chains of two antiparallel melittin protomers to form an AB dimer as in Fig. 2. We expect that this adhesion would occur when each chain has the $\sim 120^\circ$ bend between the two α -helical regions allowing close packing of the side chains from the two protomers. The final stage in the folding

pathway might either be contact between two melittin dimers or the separate addition of two chains to a dimer to form a tetramer.

Comparison of Results with Those of Nuclear Magnetic Resonance and of Circular Dichroism—The NMR studies of Brown *et al.* (3) indicated that Ile-2 side chains are in close proximity to a tryptophanyl residue in tetrameric melittin. In our model C _{δ 1} of Ile-2 in chain A is about 3 Å from C _{γ} of Trp-19 in chain B and C _{δ 1} of Ile-2 in chain B is about 4 Å from C _{γ} of Trp-19 in chain A. Brown *et al.* (3) also suggest that the C-terminal hydrophilic residues of melittin in the tetrameric state adopt an increasing variety of conformations as the temperatures is raised from 30 to 90°C while those of most of the NH₂-terminal 20 residues remain in an essentially fixed conformation. This seems reasonable because there are many interchain contacts between the hydrophobic residues in the tetramer in residues 1-20 but there are only few interchain contacts for residues 21-26. Thus, the C-terminal region can probably adopt a flexible conformation without affecting the overall packing of the tetramer.

The crystallographic results presented here agree only qualitatively with the CD measurements performed recently on tetrameric melittin. Tetrameric melittin was found to be 48% α -helical using CD (11) while we find that about 90% of the backbone of melittin can be described as α -helix. However, these CD measurements were performed at much lower salt concentrations than those used in the crystallization of melittin. Perhaps the positively charged COOH-terminal helix unwinds at low ionic strength as well as at high temperature.

Acknowledgments—We thank Drs. W. Wickner and S. G. Clarke for discussion.

REFERENCES

- Habermann, E. (1972) *Science* **177**, 314-322
- Fauçon, J. F., Dufourcq, J., and Lussan, C. (1979) *FEBS Lett.* **102**, 187-190
- Brown, L. R., Lauterwein, J., and Wüthrich, K. (1980) *Biochim. Biophys. Acta* **622**, 231-244
- Sessa, G., Freer, J. H., Colacicco, G., and Weissmann, G. (1969) *J. Biol. Chem.* **244**, 3575-3582
- Williams, J. C., and Bell, R. M. (1972) *Biochim. Biophys. Acta* **288**, 255-262
- Hegner, D., Schummer, U., and Schnepel, G. H. (1973) *Biochim. Biophys. Acta* **291**, 15-22
- Thelestam, M., and Mollby, R. (1976) *Med. Biol.* **54**, 39-49
- Verma, S. P., and Wallach, D. F. H. (1976) *Biochim. Biophys. Acta* **426**, 616-623
- Mollay, C. (1976) *FEBS Lett.* **64**, 65-68
- Dawson, C. R., Drake, A. F., Helliwell, J., and Hider, R. C. (1978) *Biochim. Biophys. Acta* **510**, 75-86
- Knöppel, E., Eisenberg, D., and Wickner, W. (1979) *Biochemistry* **18**, 4177-4181
- De Bony, J., Dufourcq, J., and Clin, B. (1979) *Biochim. Biophys. Acta* **552**, 531-534
- Lauterwein, J., Bösch, C., Brown, L. R., and Wüthrich, K. (1979) *Biochim. Biophys. Acta* **556**, 244-264
- Esser, A. F., Bartholomew, R. M., Jensen, F. C., and Müller-Eberhard, H. J. (1979) *Proc. Natl. Acad. Sci.* **76**, 5843-5847
- DeGrado, W. F., Kézdy, F. J., and Kaiser, E. T. (1981) *J. Am. Chem. Soc.* **103**, 679-681
- Mollay, C., and Kreil, G. (1974) *FEBS Lett.* **46**, 141-144
- Shier, W. T. (1979) *Proc. Natl. Acad. Sci.* **76**, 195-199
- Cole, L. J., and Shipman, W. H. (1969) *Am. J. Physiol.* **217**, 965-968
- Olson, F. C., Munjal, D., and Malviya, A. N. (1974) *Toxicon* **12**, 419-425
- Cook, G. H., and Wolff, J. (1977) *Biochim. Biophys. Acta* **498**, 255-258
- Ishay, J., Fishel, J., Rothen, F., Talmor, N., Buimovitch, B., and Asanta, M. (1977) *Toxicon* **15**, 283-291
- Tashjian, A. H., Jr., Ivey, J. L., Delclos, B., and Levine, L. (1978)

- Prostaglandins* **16**, 221-232
23. Shkenderov, S., and Koburova, K. (1979) *Toxicon* **17**, 517-519
 24. Lad, P. J., and Shier, W. T. (1979) *Biochem. Biophys. Res. Commun.* **89**, 315-321
 25. Mufson, R. A., Laskin, J. D., Fisher, P. B., and Weinstein, I. B. (1979) *Nature* **280**, 72-74
 26. Habermann, V. E., and Jentsch, J. (1967) *Hoppe-Seyler's Z. Physiol. Chem.* **348**, 37-50
 27. Anderson, D., Terwilliger, T. C., Wickner, W., and Eisenberg, D. (1980) *J. Biol. Chem.* **255**, 2578-2582
 28. Terwilliger, T. C., and Eisenberg, D. (1982) *J. Biol. Chem.* **257**, 6010-6015
 29. Terwilliger, T. C., Weissman, L., and Eisenberg, D. (1982) *Biophys. J.* **37**, 353-361
 30. Richards, F. M. (1974). *J. Mol. Biol.* **82**, 1-14
 31. Eisenberg, D. S., Terwilliger, T. C., and Tsui, F. C. (1980) *Biophys. J.* **32**, 252-254
 32. Weast, R. C. (ed). (1979) *C. R. C. Handbook of Chemistry and Physics*, p. C-270, CRC Press, Boca Rata, FL
 33. Chothia, C., Levitt, M., and Richardson, D. (1981) *J. Mol. Biol.* **145**, 215-250
 34. Weber, P. C., and Salemme, F. R. (1980) *Nature* **287**, 82-84
 35. Snodgrass, R. E. *Anatomy of the Honeybee* (1956) Comstock Publishing Associates, Ithaca, NY
 36. Kreil, G., and Bachmayer, H. (1971) *Eur. J. Biochem.* **20**, 344-350
 37. Habermann, E., and Kowallek, H. (1970) *Hoppe-Seyler's Z. Physiol. Chem.* **351**, 884-890
 38. Lauterwein, J., Brown, L. R., and Wüthrich, K. (1980) *Biochim. Biophys. Acta* **622**, 219-230